Photon shot noise dephasing in the strong-dispersive limit of circuit QED

A. P. Sears, A. Petrenko, G. Catelani, L. Sun, Hanhee Paik, G. Kirchmair, L. Frunzio, L. I. Glazman, S. M. Girvin, and R. J. Schoelkopf

Phys. Rev. B **86**, 180504 — Published 12 November 2012

DOI: 10.1103/PhysRevB.86.180504

Photon Shot Noise Dephasing in the Strong-Dispersive Limit of Circuit QED

A. P. Sears, A. Petrenko, G. Catelani, L. Sun, Hanhee Paik, G. Kirchmair, L. Frunzio, L. I. Glazman, S. M. Girvin, and R. J. Schoelkopf
Department of Physics and Applied Physics, Yale University, New Haven, Connecticut 06520, USA
(Dated: October 25, 2012)

We study the photon shot noise dephasing of a superconducting transmon qubit in the strong-dispersive limit, due to the coupling of the qubit to its readout cavity. As each random arrival or departure of a photon is expected to completely dephase the qubit, we can control the rate at which the qubit experiences dephasing events by varying *in situ* the cavity mode population and decay rate. This allows us to verify a pure dephasing mechanism that matches theoretical predictions, and in fact explains the increased dephasing seen in recent transmon experiments as a function of cryostat temperature. We observe large increases in coherence times as the cavity is decoupled from the environment, and after implementing filtering find that the intrinsic coherence of small Josephson junctions when corrected with a single Hahn echo is greater than several hundred microseconds. Similar filtering and thermalization may be important for other qubit designs in order to prevent photon shot noise from becoming the dominant source of dephasing.

PACS numbers: 03.67.Lx, 42.50.Pq, 85.25

Rapid progress[1–3] is being made in engineering superconducting qubits and effectively isolating them from the surrounding electromagnetic environment, often through the use of resonant cavities. When coupled dispersively, for example when used for a quantum bus or memory, changes in oscillator occupation can shift the qubit energy, leading to an unintended measurement of the qubit and a loss of coherence.

Recently[4] superconducting qubits have been created inside a three-dimensional (3D) resonator, leading to more than an order of magnitude increase in coherence time. Interestingly, the energy relaxation time T_1 has increased even more than the phase coherence time T_2^*, pointing to a new or newly important mechanism for dephasing[5]. These devices have a single Josephson junction, eliminating the sensitivity to flux noise[6], and surprisingly show only a weak temperature-dependent dephasing, inconsistent with some predictions based on extrapolations of junction critical current noise[7,8]. In these devices, the qubit state is detected by observing the dispersive frequency shift of a resonant cavity. However, it is known[9–11] that in the strong-dispersive regime the qubit becomes very sensitive to stray cavity photons, which cause dephasing due to their random ac-Stark shift[12]. It requires increasing care to prevent this extrinsic mechanism from becoming the dominant source of dephasing as qubit lifetimes increase. Experiments elsewhere[13] and in our lab have shown that pure dephasing times can be many hundreds of microseconds after careful thermalization and more extensive filtering.

In this Letter, we quantitatively test the dephasing of a qubit due to photon shot noise in the strong-dispersive coupling limit with a cavity. In this novel regime where the ac-Stark shift per photon is many times greater than the qubit linewidth γ and the cavity decay rate κ[14], the passage of any photon through the cavity performs a complete and unintended measurement of the qubit state. This limit also allows a precise determination of the photon number in the cavity using Rabi experiments on the photon number-split qubit spectrum[15]. With a simulated thermal bath injecting photons into the cavity and *in situ* mechanical adjustment of the cavity κ, we find a pure dephasing of the qubit that quantitatively matches theory[10]. Furthermore, we verify that the qubit is strongly coupled to photons in several cavity modes and find that the dephasing from these modes accounts for the reduced coherence times as a function of cryostat temperature. Our measurements at 10 mK demonstrate that decreasing κ leads to longer qubit coherence times, suggesting that existing dephasing in superconducting qubits is due to unintended and preventable measurement by excess photons in higher frequency modes.

The experiments were performed (see Fig. 1a) with a transmon qubit coupled in the strong-dispersive limit to a 3D cavity, and well approximated by the Hamiltonian[16]:

$$\mathrm{H_{eff}}/\hbar = \omega_c a^\dagger a + \left(\omega_q - \chi a^\dagger a\right) b^\dagger b - \frac{\alpha}{2} b^\dagger b^\dagger b b, \tag{1}$$

where the operator $a^\dagger$ creates a cavity photon and the operator $b^\dagger$ creates a qubit excitation. Then ω_c is the cavity frequency, ω_q and α are the qubit frequency (fixed and far detuned from the cavity) and anharmonicity, and $\chi/2\pi = 7$ MHz is the light shift per photon which can be 1000 times larger than the qubit linewidth of $\gamma/2\pi = 5-12$ kHz, and the cavity linewidth $\kappa/2\pi = 6-120$ kHz. The large dispersive shift leads to the well-resolved peaks in the qubit spectrum (see Fig. 1b-c), allowing us to conditionally manipulate the qubit depending on the cavity photon number N[15]. Measuring the height of a given photon number-split qubit peak (or the amplitude of a Rabi oscillation at frequency $\omega_q - N\chi$) allows a direct determination of the probability $P(N)$ for the cavity to have a particular photon number.

Dephasing of the qubit can be caused by a random change in cavity photon number, which shifts the qubit energy by $\hbar\chi$ per photon and leads to a large rate of phase accumulation relative to γ. Then the pure dephasing rate γ_ϕ, obtained in a Ramsey

experiment for the qubit, depends on the stability of the N photon cavity state. When the cavity is connected to a thermal bath, the probability $P(N)$ follows a system of equations[17] for the rate of change into and out of the N photon state: $dP(N)/dt = \kappa(\bar{n}+1)(N+1)P(N+1) + \kappa\bar{n}NP(N-1) - \Gamma_{\rm out}P(N)$, where the cavity decay rate $\kappa = 1/\tau$ is the inverse of its decay time τ, $\bar{n}$ is the average number of photons, and

$$\Gamma_{\rm out} = \kappa[(\bar{n}+1)N + \bar{n}(N+1)] \tag{2}$$

combines the spontaneous emission of photons with the stimulated emission due to thermal photons. Then, in the strong-dispersive regime (and neglecting other sources of dephasing) the dephasing rate becomes $\gamma_\phi = \Gamma_{\rm out}$, and the success of an experiment that relies on phase predictability of the qubit requires a constant photon number in the cavity throughout each cycle.

To verify this prediction for γ_ϕ quantitatively, we first calibrate our thermal bath and then obtain κ with experiments on the photon peaks of the qubit. We can determine the cavity decay rate κ by exciting the cavity with a short coherent pulse while measuring the repopulation of the ground state $|{\rm g},0\rangle$ (i.e. the amplitude of the zero-photon Rabi oscillations) over timescale τ. Alternatively, exciting the cavity with a wideband noise source that covers the cavity ω_c transition frequency but not the qubit ω_q transition frequency, creates an average photon number $\bar{n} = AP_{BE}(T)Q/Q_c$, as shown in the Supplement[18] (see, also, references[4,19–24] therein) . Here, A is the linear power loss from additional cold attenuation, $P_{BE} = 1/(e^{\hbar\omega/kT}-1)$ is the Bose-Einstein population of the 50 Ω load of the noise source at effective temperature T, located outside the cavity. The total cavity quality factor $Q = \omega_c\tau$ has an inverse which is the sum of the inverses of the coupling quality factor Q_c of the noise source port, all other port couplings, and the internal quality factor $Q_{\rm int}$. In steady state and for uncorrelated noise, the probability $P(N)$ of finding the qubit in an environment with N photons is a thermal distribution $P(N) = \bar{n}^N/(\bar{n}+1)^{(N+1)}$, as verified by the data in Fig. 1d. With these measurements we obtain the scaling of $\bar{n}$ as a function of applied noise power for each different value of κ, allowing a comparison with Eq. 2 using no adjustable parameters.

To observe the influence of photon dephasing on our qubit, we test Eq. 2 over a wide range of values for both $\bar{n}$ and κ as shown in Fig. 2. The photon number is varied by adjusting the attenuation following our noise source, while κ is controlled by retracting the resonator output coupler using a Kevlar string connected to the top of the fridge, exponentially increasing the Q_c as it is withdrawn. For large κ, photons enter and leave quickly, so long periods uninterrupted by a transit are rare even if the average occupation is low, and the phase coherence time is short. In the Ramsey data shown in Fig. 2 the dephasing rate is universally proportional to injected $\bar{n}$ and κ, with an offset due to spontaneous decay (if $N > 0$), and residual photons or other intrinsic dephasing. These experiments confirm our understanding of the qubit dephasing rate in the strong-dispersive limit, and point to the importance of excess photons or an effective temperature of a mode for qubit coherence.

Importantly, we use slow Gaussian pulses to control the qubit in order to exploit the photon-dependence of our Hamiltonian. With a width of $\sigma = 100$ ns, the narrow frequency span of the pulses means that Ramsey experiments add signal contrast only when the chosen photon number N has remained in the cavity throughout the experiment, a type of post-selection evident in the different scalings of Fig. 2b-d. Once conditioned, photon transitions during the experiment lead to an incoherent response in our qubit readout, when at a random point in time t_0 an initially prepared superposition changes: $|\psi(t_0)\rangle = 1/\sqrt{2}(|{\rm g},0\rangle + |{\rm e},0\rangle) \rightarrow |\psi(t)\rangle = 1/\sqrt{2}(|{\rm g},1\rangle + \exp[i\chi(t-t_0)]\,|{\rm e},1\rangle)$ for time $t > t_0$. Our qubit readout[25] traces over all photon states, while a photon number change entangles the qubit with a degree of freedom which is discarded or produces a superposition with unknown final phase, leading to a decay in the Ramsey fringes as the experiment records the qubit excitation despite any cavity transition. Additionally, a characteristic bump and slope are visible in the data and must be removed before fitting the Ramsey signal with the usual decaying sine function. These features can be understood as the re-equilibration of the cavity photon number after the first qubit manipulation conditionally prepares a certain photon number, and are well fit (see Fig. 3 of the Supplement) by a simple master equation which includes the incoherent cavity drive as well as qubit and cavity decay.

While the fundamental ${\rm TE}_{101}$ mode of our 3D resonator serves both as the qubit readout channel and as a mechanism for dephasing, the rectangular cavity in fact supports a set of ${\rm TE}_{10n}$ modes[26] whose influence we must consider. Then a more comprehensive Hamiltonian than Eq. 1 must incorporate many different cavity frequencies, each with a coupling strength that depends on antenna length and the positioning of the qubit in the cavity[16]. This coupling g_n is large for odd-n ${\rm TE}_{10n}$ modes where the electric field has an antinode at the qubit, while the even-n modes have greatly diminished coupling to the qubit due to a node along the qubit antenna. For our parameters, the fundamental ${\rm TE}_{101}$ mode $\omega_1/2\pi = 8.01$ GHz, $\omega_q/2\pi = 6.65$ GHz, and $g_1/2\pi = 127$ MHz, the qubit anharmonicity $\alpha = 340$ MHz leads to an ac-Stark shift of $\chi_1/2\pi = 7$ MHz. Similarly, the first odd harmonics ${\rm TE}_{103}$ with $\omega_3 = 12.8$ GHz has a large $\chi_3/2\pi = 1$ MHz. In fact, with this mode we can perform high fidelity readout, measure the photon mode population (using longer $\sigma = 800$ ns width pulses), and observe its influence on decoherence by injecting noise near ω_3. In general, we should consider *all* cavity modes that have a non-zero coupling to the qubit as sources of significant decoherence. For example, the odd-n ${\rm TE}_{10n}$ modes at frequency ω_n and detuning $\Delta_n = \omega_n - \omega_q$, have a coupling $g_n \propto \sqrt{\omega_n}$ and an ac-Stark shift $\chi_n = g_n^2\alpha/\Delta_n(\Delta_n+\alpha)$ which decrease only slowly as $1/n$. Consequently, there may be many modes with significant dispersive shifts that can act as sources of extrinisic qubit decoherence. Moreover, since the coupling quality factors of these modes typically decreases with frequency, even very small photon occupancies (which are usually ignored, not measured or as carefully filtered) must be suppressed to obtain maximum coherence.

The photon shot noise from multiple cavity modes provides a simple explanation for the anomalous qubit dephasing previously observed[4] as a function of cryostat temperature. In this case, each cavity mode should be populated with the Bose-Einstein

probability P_{BE} and these thermal photons can make an unintended measurement of the qubit, disrupting phase-sensitive experiments. The predicted occupancies for the TE_{101} and TE_{103} modes are shown (green lines) in the inset of Fig. 3, along with their predicted dephasing (blue lines). Having confirmed the dephasing rates for all modes individually we can now combine the effect of all modes that strongly couple to the qubit: $\gamma_\phi = \sum \bar{n}_i \kappa_i$. This total thermal decoherence rate is shown as the red dashed line in the inset of Fig. 3, for typical parameters. Since these modes have $\hbar\omega_n \gg k_B T$, the predicted dephasing time is in excess of 100 microseconds below 80 mK due to the exponentially suppressed number of blackbody photons. However, since any particular mode coupling to the qubit in the strong-dispersive limit may have a relatively fast decay time τ, even very small ($\sim 10^{-3} - 10^{-2}$) non-thermal populations $\bar{n}$ could easily satisfy $\bar{n}\kappa \gg 1/2T_1$, limiting the coherence through pure dephasing alone to $T_2^* \approx 1/\gamma_\phi = \tau/\bar{n}$. The measured coherence times as a function of temperature are well fit (see Fig. 3) by the combined dephasing of thermal occupancy of the TE_{101} and TE_{103} modes, plus a parameter adjusted to represent the residual dephasing in each experiment. This excess could be due to another mechanism intrinsic to the qubit, or simply due to insufficient filtering or thermalization of the apparatus, leading to a small non-thermal photon population.

Further evidence that the intrinsic coherence limits of the 3D transmons at millikelvin temperatures have not yet been observed is provided by the data shown in Fig. 4, where the qubit relaxation time (T_1), Ramsey time (T_2^*), and Hahn echo time (T_{2E}) at 10 mK are shown as a function of the TE_{101} cavity decay time. The relaxation time is relatively unaffected by cavity lifetime, since this qubit is sufficiently detuned from the cavity to minimize the Purcell effect[1]. However, we observe a general trend where T_2^* and T_{2E} increase as the cavity lifetime increases, consistent with a decoherence due to residual photons with ever slower dynamics, but *not* expected due to e.g. junction critical current noise, which should be independent of cavity properties. With the addition of absorptive[23,27] and reflective[24] low-pass filters which cover the TE_{103} and higher frequencies, a similar device (see the Supplement) experienced a drop of cavity population from 3% to less than 0.2%. Our devices are sometimes affected by an unexplained low-frequency noise (perhaps due to charge dispersion), so we find it informative to include a single Hahn echo in our Ramsey experiments. The measured value of this dephasing time with echo increased in the filtered configuration from 75 μs to 800 μs (with T_1 going from 28 μs to 48 μs and T_{2E} from 32 μs to 87 μs), suggesting that proper heat-sinking and filtering components can effectively eliminate photon dephasing.

In conclusion, we have performed experiments involving precise thermal photon populations to quantitatively induce qubit dephasing in good agreement with simple theory. We find that photons in the fundamental and at least one harmonic mode of the cavity strongly couple to a transmon qubit and note that at the nominal base temperature of our cryostat they produce a negligible amount of dephasing. However, the sensitivity of the qubit to photons at many frequencies requires that we either keep all modes of the cavity in their ground state, or else minimize the influence of non-thermal populations by reducing their measurement rate[28]. Inclusion of the cavity harmonics in dephasing calculations leads to an understanding of the earlier, anomalous, temperature-dependent decoherence in our devices[4]. Finally, we find evidence that interactions with the residual photons in our 3D cavity likely mask the intrinsic coherence time of the Josephson junction, a concern that is relevant for superconducting qubit designs[29,30], quantum dots[31], and more generally any Quantum Information system coupled to a bosonic mode[32]. As qubit linewidths shrink in the future, other effects such as quasiparticle parity[33–35] or interactions with nuclear spins[36] may further split the qubit spectrum, enabling probes of their state dynamics using these procedures.

We thank Michel Devoret for valuable discussions. L. F. acknowledges partial support from CNR-Istituto di Cibernetica. This research was funded by the Office of the Director of National Intelligence (ODNI), Intelligence Advanced Research Projects Activity (IARPA), through the Army Research Office, as well as by the National Science Foundation (NSF DMR-1004406). L. G. acknowledges support from NSF DMR Grant No 12066121.

[1] A. Houck, J. Schreier, B. Johnson, J. Chow, J. Koch, J. Gambetta, D. Schuster, L. Frunzio, M. Devoret, S. Girvin, et al., Physical Review Letters **101**, 080502 (2008).
[2] M. Neeley, M. Ansmann, R. C. Bialczak, M. Hofheinz, N. Katz, E. Lucero, A. OConnell, H. Wang, A. N. Cleland, and J. M. Martinis, Physical Review B **77**, 180508(R) (2008).
[3] M. Steffen, F. Brito, D. DiVincenzo, S. Kumar, and M. Ketchen, New Journal of Physics **11**, 033030 (2009).
[4] H. Paik, D. Schuster, L. Bishop, G. Kirchmair, G. Catelani, A. Sears, B. Johnson, M. Reagor, L. Frunzio, L. Glazman, et al., Physical Review Letters **107**, 240501 (2011).
[5] A. A. Houck, J. Koch, M. H. Devoret, S. M. Girvin, and R. J. Schoelkopf, Quantum Information Processing **8**, 105 (2009).
[6] F. C. Wellstood, C. Urbina, and J. Clarke, Applied Physics Letters **50**, 772 (1987).
[7] D. J. Van Harlingen, T. L. Robertson, B. L. T. Plourde, P. A. Reichardt, T. A. Crane, and J. Clarke, Physical Review B **70**, 064517 (2004).
[8] J. Eroms, L. C. van Schaarenburg, E. F. C. Driessen, J. H. Plantenberg, C. M. Huizinga, R. N. Schouten, A. H. Verbruggen, C. J. P. M. Harmans, and J. E. Mooij, Applied Physics Letters **89**, 122516 (2006).
[9] P. Bertet, I. Chiorescu, G. Burkard, K. Semba, C. J. P. M. Harmans, D. P. DiVincenzo, and J. E. Mooij, Physical Review Letters **95**, 257002 (2005).
[10] J. Gambetta, A. Blais, D. I. Schuster, A. Wallraff, L. Frunzio, J. Majer, M. H. Devoret, S. M. Girvin, and R. J. Schoelkopf, Physical Review A **74**, 042318 (2006).
[11] I. Serban, E. Solano, and F. K. Wilhelm, Europhysics Letters (EPL) **80**, 40011 (2007).

[12] D. I. Schuster, A. Wallraff, A. Blais, L. Frunzio, R. S. Huang, J. Majer, S. M. Girvin, and R. J. Schoelkopf, Physical Review Letters **94**, 123602 (2005).
[13] C. Rigetti, J. Gambetta, S. Poletto, B. Plourde, J. Chow, A. Corcoles, J. Smolin, S. Merkel, J. Rozen, G. Keefe, et al., Physical Review B **86**, 100506 (2012).
[14] D. I. Schuster, A. A. Houck, J. A. Schreier, A. Wallraff, J. M. Gambetta, A. Blais, L. Frunzio, J. Majer, B. Johnson, M. H. Devoret, et al., Nature **445**, 515 (2007).
[15] B. R. Johnson, M. D. Reed, A. A. Houck, D. I. Schuster, L. S. Bishop, E. Ginossar, J. M. Gambetta, L. DiCarlo, L. Frunzio, S. M. Girvin, et al., Nature Physics **6**, 663 (2010).
[16] S. E. Nigg, H. Paik, B. Vlastakis, G. Kirchmair, S. Shankar, L. Frunzio, M. H. Devoret, R. J. Schoelkopf, and S. M. Girvin, Physical Review Letters **108**, 240502 (2012).
[17] D. F. Walls and G. J. Milburn, *Quantum optics* (Springer, Berlin; New York, 1994), ISBN 3540588310.
[18] See the Supplemental Materials for model and additional data
[19] A. D. Corcoles, J. M. Chow, J. M. Gambetta, C. Rigetti, J. R. Rozen, G. A. Keefe, M. Beth Rothwell, M. B. Ketchen, and M. Steffen, Applied Physics Letters **99**, 181906 (2011).
[20] N. Ramsey, *Molecular beams* (Clarendon Press ; Oxford University Press, Oxford; New York, 1985), ISBN 0198520212.
[21] M. Goppl, A. Fragner, M. Baur, R. Bianchetti, S. Filipp, J. M. Fink, P. J. Leek, G. Puebla, L. Steffen, and A. Wallraff, Journal of Applied Physics **104**, 113904 (2008).
[22] F. Pobell, *Matter and methods at low temperatures* (Springer-Verlag, Berlin; New York, 1996), ISBN 3540585729.
[23] D. F. Santavicca and D. E. Prober, Measurement Science and Technology **19**, 087001 (2008).
[24] K&L 6L250-10000/T20000-OP/O, http://www.klmicrowave.com/.
[25] M. D. Reed, L. DiCarlo, B. R. Johnson, L. Sun, D. I. Schuster, L. Frunzio, and R. J. Schoelkopf, Physical Review Letters **105**, 173601 (2010).
[26] C. P. Poole, *Electron spin resonance : a comprehensive treatise on experimental techniques* (Wiley, New York [u.a.], 1967), ISBN 9780470693865.
[27] D. H. Slichter, O. Naaman, and I. Siddiqi, Applied Physics Letters **94**, 192508 (2009).
[28] S. Shankar and M. Hatridge in prep.
[29] A. A. Abdumalikov, O. Astafiev, Y. Nakamura, Y. A. Pashkin, and J. S. Tsai, Physical Review B **78**, 180502 (2008).
[30] M. S. Allman, F. Altomare, J. D. Whittaker, K. Cicak, D. Li, A. Sirois, J. Strong, J. D. Teufel, and R. W. Simmonds, Physical Review Letters **104**, 177004 (2010).
[31] T. Frey, P. J. Leek, M. Beck, A. Blais, T. Ihn, K. Ensslin, and A. Wallraff, Physical Review Letters **108**, 046807 (2012).
[32] M. Brune, F. Schmidt-Kaler, A. Maali, J. Dreyer, E. Hagley, J. M. Raimond, and S. Haroche, Physical Review Letters **76**, 1800 (1996).
[33] J. Schreier, A. Houck, J. Koch, D. Schuster, B. Johnson, J. Chow, J. Gambetta, J. Majer, L. Frunzio, M. Devoret, et al., Physical Review B **77**, 180502(R) (2008).
[34] L. Sun, L. DiCarlo, M. Reed, G. Catelani, L. Bishop, D. Schuster, B. Johnson, G. Yang, L. Frunzio, L. Glazman, et al., Physical Review Letters **108**, 230509 (2012).
[35] O. Naaman and J. Aumentado, Physical Review B **73**, 172504 (2006).
[36] D. Schuster, A. Sears, E. Ginossar, L. DiCarlo, L. Frunzio, J. Morton, H. Wu, G. Briggs, B. Buckley, D. Awschalom, et al., Physical Review Letters **105**, 140501 (2010).
[37] G. Catelani, J. Koch, L. Frunzio, R. J. Schoelkopf, M. H. Devoret, and L. I. Glazman, Physical Review Letters **106**, 077002 (2011).

CAPTIONS

FIG. 1: (a) Experimental setup (see also the Supplement). Noise of varying amplitude at the cavity transition frequency is sent into the input port of a 3D resonator. The output port of the resonator has a movable coupler which varies the output side coupling quality factor Q_c from 1.0×10^5 to 2.5×10^7. (b) Energy level diagram. The qubit has a transition frequency that is ac-Stark shifted by $-\chi$ for each photon in the cavity. (c) Photon number-splitting of the qubit spectrum. We inject noise and create a mean number $\bar{n}$ of photons in the fundamental mode. The peaks correspond to $N=0$,1,2 photons from right to left, with the cavity $Q=1\times10^6$, and (*) even without applied noise we measure a photon occupation in the TE_{101} mode of the cavity to be $\bar{n}\sim0.02$. (d) Cavity population. Rabi experiments (shown in the Supplement) performed on each photon peak N for increasing noise power with cavity $Q=2.5\times10^5$. The signal amplitude gives the probability of finding N photons in the cavity. Two linear scaling factors, fit globally, provide conversion from homodyne readout voltage[25] to probability (vertical axis), and from attowatts within the cavity bandwidth to $\bar{n}$ (horizontal axis). Error bars represent 1σ fluctuations in the $|e\rangle$ state readout voltage. The solid lines are a thermal distribution using the fit scaling parameters.

FIG. 2: Qubit dephasing due to photon noise. (a) Qubit coherence time, determined from Ramsey experiments on the $N=0$ or $N=1$ ($\triangle$) photon peaks, as a function of both cavity Q and $\bar{n}$. The dashed lines are theory, with an offset due to residual dephasing. Each has a slope proportional to κ (or 3κ for $N=1$ experiments), according to Eq. 2. The ($\circ$) are coherence times vs. population in TE_{103} mode, which also dephases the qubit. (b) Ramsey with no noise injected, fundamental mode $Q=1\times10^6$, and $T_2^*=26$ μs. The solid line is a fit with an exponentially decaying sine. (c) A Ramsey with moderate noise. Contrast and T_2^* are reduced. Fundamental mode $Q=2.5\times10^5$, $\bar{n}=0.25$, $T_2^*=7.7$ μs. (d) Ramsey with high noise. Fundamental mode $Q=1\times10^6$, $\bar{n}=3.1$, $T_2^*=5.2$ μs. Our selective ($N=0$) pulses produce a loss of contrast and a non-oscillating signal addition (orange) as photon population returns to a thermal distribution. The dashed black line is a numerical simulation (see the Supplemental Materials).

FIG. 3: (a) Decoherence due to thermal photons. The coherence times extracted from Ramsey (T_2^*) and Hahn echo (T_{2E}) experiments measured as a function of cryostat temperature. To model dephasing (dashed lines), we predict population in the TE_{101} and TE_{103} modes of the cavity. Then, we sum the total dephasing rate using the measured quality factors for each mode (High Q: $\tau_{101}=20$ μs, $\tau_{103}=4$ μs; Low Q: $\tau_{101}=2$ μs, $\tau_{103}=400$ ns). For high Q, the use of a Hahn echo pulse leads to a large T_{2E} because either the photon state has much longer correlation time or the remaining dephasing similarly occurs at low frequencies. Although the decline in T_1 (not shown)[37] contributes to the trend, population in both TE_{101} and TE_{103} are needed for a good fit. (b) Bose-Einstein population of the first two odd-n TE_{10n} modes at 8 and 12.8 GHz (green, A and B respectively) and the coherence limits they impose individually (blue) and collectively (dashed red) for the low Q values measured above.

FIG. 4: Coherence times versus TE_{101} mode decay τ. The TE_{103} cavity, which naturally decays more strongly through the couplers, increases in Q as the entire resonator is decoupled from our coaxial lines. While T_1 is nearly constant due to the large qubit detuning from the cavity, its T_2^* and T_{2E} increase as the coupling pin is withdrawn from the 3D resonator. This is consistent with diminishing dephasing from cavity modes with $\kappa<\chi$, where a photon transit strongly measures[11] the qubit state.

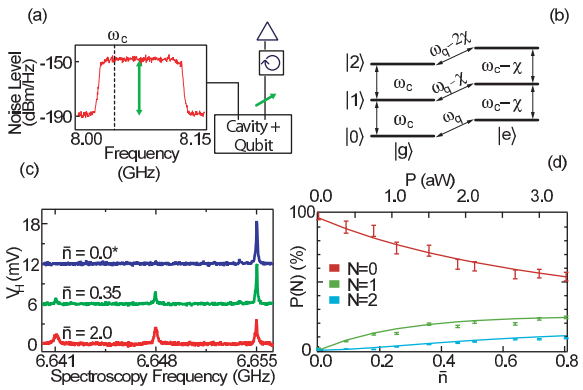

Figure 1 LT13152BR 25Oct2012

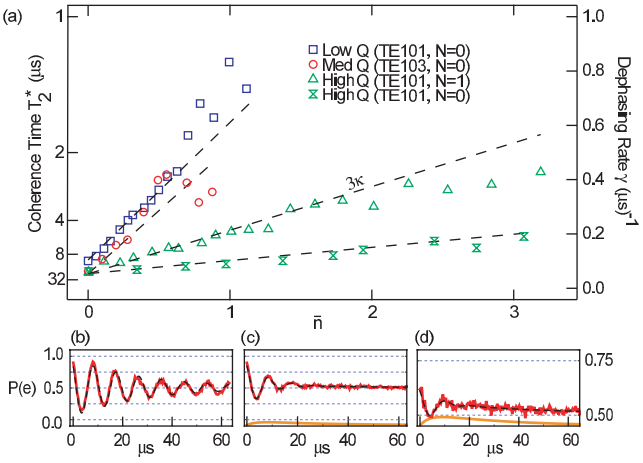

Figure 2 LT13152BR 25Oct2012

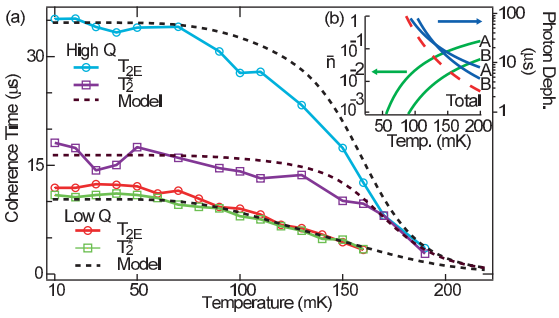

Figure 3 LT13152BR 25Oct2012

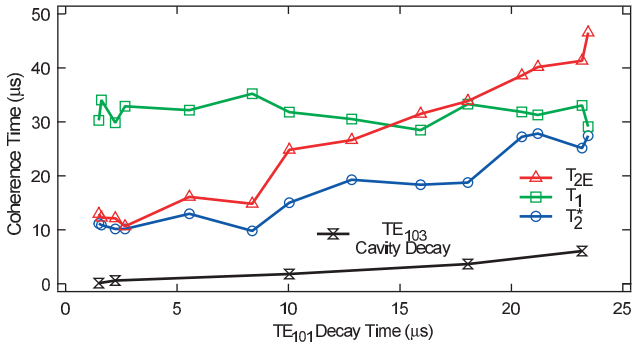

Figure 4 LT13152BR 25Oct2012